Cell Reports, Volume *24*

Supplemental Information

A Membrane Potential- and Calpain-Dependent Reversal of Caspase-1 Inhibition Regulates Canonical NLRP3 Inflammasome

Yifei Zhang, Hua Rong, Fang-Xiong Zhang, Kun Wu, Libing Mu, Junchen Meng, Bailong Xiao, Gerald W. Zamponi, and Yan Shi

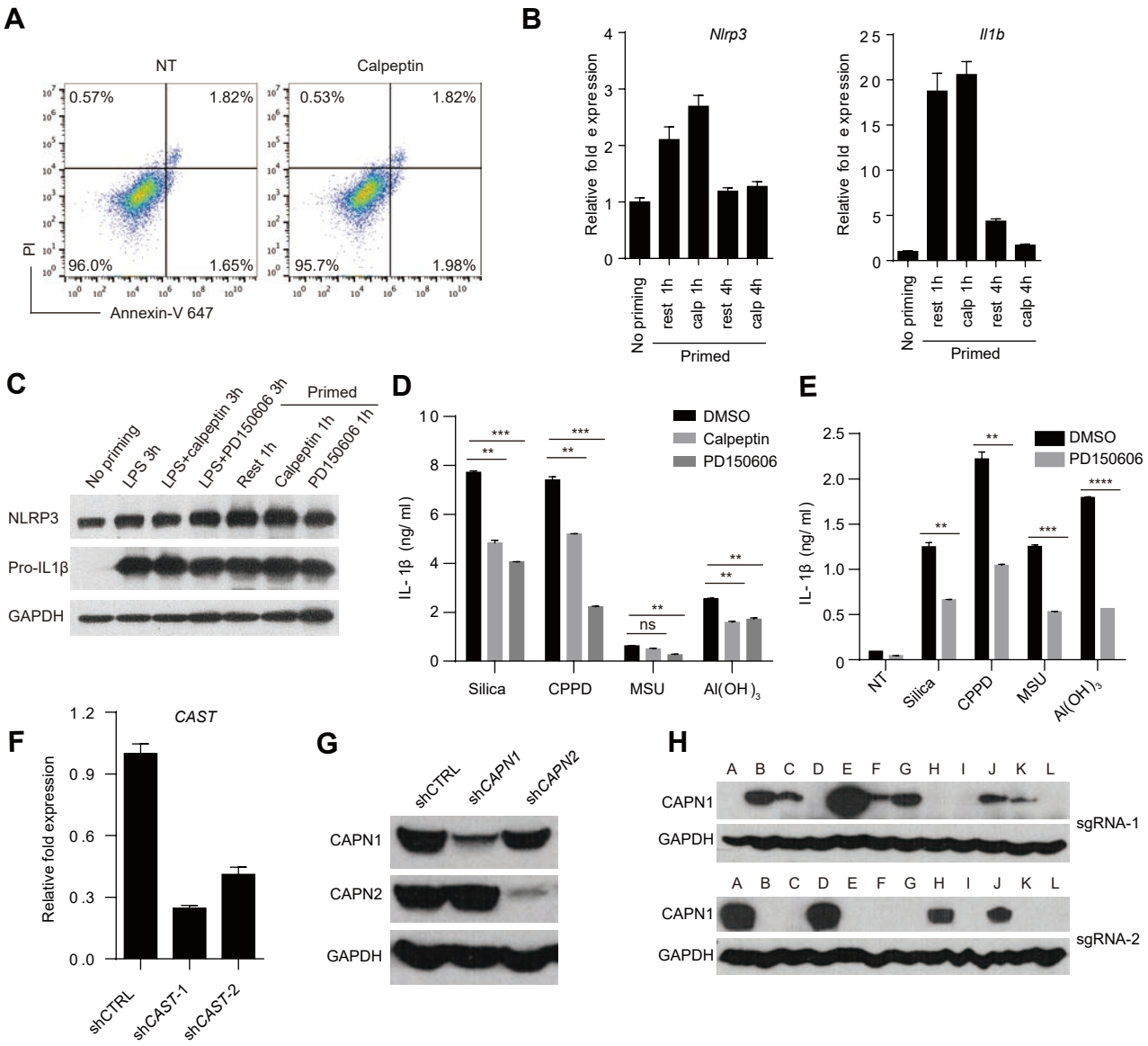

Figure S1. Calpain inhibition impairs NLRP3 inflammasome without affecting cell viability or the priming step, related to Figure 1.

(A) Flow cytometric analysis of Annexin V and PI staining in BMDCs treated with calpeptin for 6 hrs. (B) BMDCs were primed with LPS for 3 hrs and changed to fresh medium with or without calpeptin (calp) for another 1 or 4 hrs. cDNA was extracted for q-PCR analysis of NLRP3 and pro-IL-1β mRNA fold changes. (C) Calpain inhibitors were added together with LPS or after LPS priming in BMDCs. Cell lysis were subjected to WB. (D, E) ELISA analysis of IL-1β production in BMDMs (D) and THP-1 cells (E) treated with different crystals in the presence or absence of calpeptin or PD150606. (F) qPCR analysis of calpastatin (CAST) mRNA fold expression in CAST knockdown or non-targeting shRNA-treated control THP-1 cells. (G) CAPN1 and CAPN2 shRNA knockdown efficiency in THP-1 was confirmed by western blot. (H) CAPN1-deficient THP-1 clones generated with 2 different small guide RNA (sgRNA) by CRISPR-Cas9 were identified by Western blot. Data represents at least 2 independent experiments (A-E).

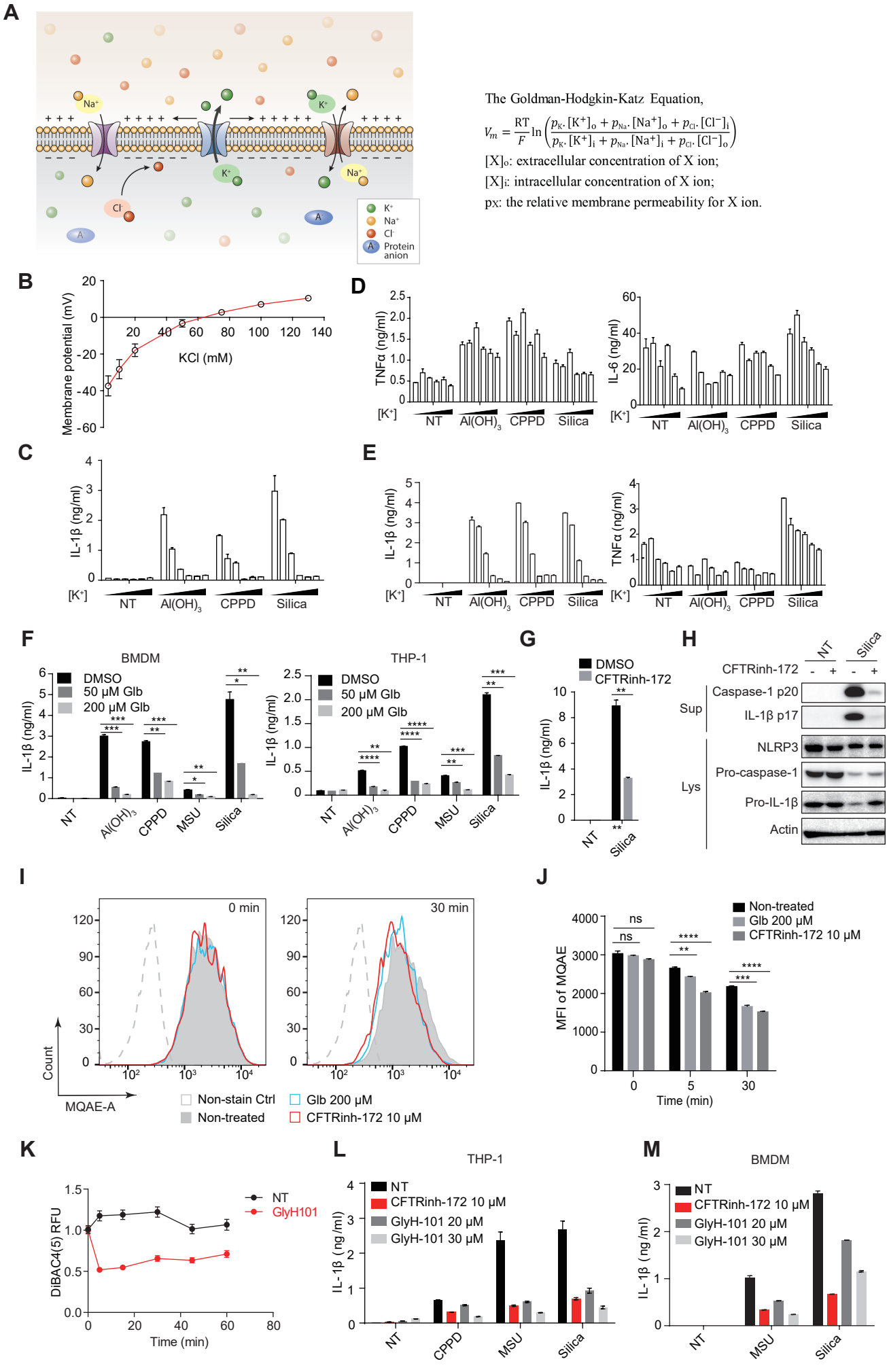
A
Na+
K+
Cl-
A-
Protein anion
The Goldman-Hodgkin-Katz Equation,
$V_m = \frac{RT}{F}\ln\left(\frac{p_K.[K^+]_o + p_{Na}.[Na^+]_o + p_{Cl}.[Cl^-]_i}{p_K.[K^+]_i + p_{Na}.[Na^+]_i + p_{Cl}.[Cl^-]_o}\right)$
[X]o: extracellular concentration of X ion;
[X]i: intracellular concentration of X ion;
px: the relative membrane permeability for X ion.
B
Membrane potential (mV)
KCl (mM)
C
IL-1β (ng/ml)
[K+]
NT
Al(OH)3
CPPD
Silica
D
TNFα (ng/ml)
IL-6 (ng/ml)
E
IL-1β (ng/ml)
TNFα (ng/ml)
F
BMDM
THP-1
DMSO
50 μM Glb
200 μM Glb
MSU
G
DMSO
CFTRinh-172
H
NT
Silica
CFTRinh-172
Sup
Caspase-1 p20
IL-1β p17
Lys
NLRP3
Pro-caspase-1
Pro-IL-1β
Actin
I
0 min
30 min
Count
MQAE-A
Non-stain Ctrl
Non-treated
Glb 200 μM
CFTRinh-172 10 μM
J
MFI of MQAE
Non-treated
Glb 200 μM
CFTRinh-172 10 μM
Time (min)
K
DiBAC4(5) RFU
NT
GlyH101
Time (min)
L
THP-1
NT
CFTRinh-172 10 μM
GlyH-101 20 μM
GlyH-101 30 μM
IL-1β (ng/ml)
M
BMDM

Figure S2. Depolarization or hyperpolarization of membrane potential impairs IL-1β production but not dramatically affect caspase-1 independent cytokine secretion, related to Figure 2.
(A) According to the Goldman-Hodgkin-Katz Equation, K^+, Na^+, and Cl^- are the main contributors to the membrane potential. The MP depends on not only the concentration gradients of those ions, but also their relative membrane permeability. In the resting state, the outward movement of K^+ driven by chemical diffusion sets up a positive charge at the external membrane interface. This is countered by the accumu lation of Cl^- near the inner leaflet interface. This creates the resting MP for all eukaryotic cells. In a typical experimental setting, increased extracellular K^+ concentrations with reciprocal reduction of Na^+ to keep osmolarity constant results in MP depolarization because in most cells the resting p K (permeability of K^+) is larger than p Na or p Cl. On the other hand, inhibition of chloride ion channels by glyburide or CFTRinh-172, will cause Cl^- accumulation inside the cell and MP hyperpolarization. (B) BMDCs MP in response to different K^+ concentrations (n=6). (C, D) BMDCs were treated with different crystals in different concentrations of extracellular K^+ (5, 10, 20, 50, 75 and 100 mM, left to right). IL-1β (C), TNFα and IL-6 (D) in supernatants were measured by ELISA after 5 hrs (n=3). (E) ELISA analysis for IL-1β and TNFα secretion in BMDMs treated with different crystals in different concentrations of K^+ (5, 10, 20, 50, 75 and 100 mM, left to right). (F) ELISA analysis of IL-1β secreted by BMDMs or THP-1 stimulated with different crystals in the presence or absence of glyburide (Glb). (G) Elisa analysis of IL-1β production in BMDMs treated with different crystals in the presence or absence of CFTRinh-172. (H) Immunoblot of activated Caspase-1 and mature IL-1β in supernatants (Sup) and all NLRP3 inflammasome components in cell lysates (Lys) of BMDMs. (I, J) Intracellular chloride ion concentration changes in response to glyburide and CFTRinh-172 were measured by MAQE staining on flow cytometer. The fluorescent intensity of MQAE decreases in proportion to the chloride increase in cells (n=3). (K) Changes of MP of THP-1 cells under GlyH-101 treatment or DMSO control were measured by DiBAC4(5) staining. Each point was mean ± SEM of cells from at least 12 fields in 2 independent experiments. (L and M) ELISA analysis of IL-1β in supernatants from THP-1 cells (L) or BMDMs (M) stimulated with different crystals in the presence or absence of CFTRinh-172 or GlyH-101. Results are representative of at least of three independent experiments (C-G, J, L and M, mean ± SEM, n=3).

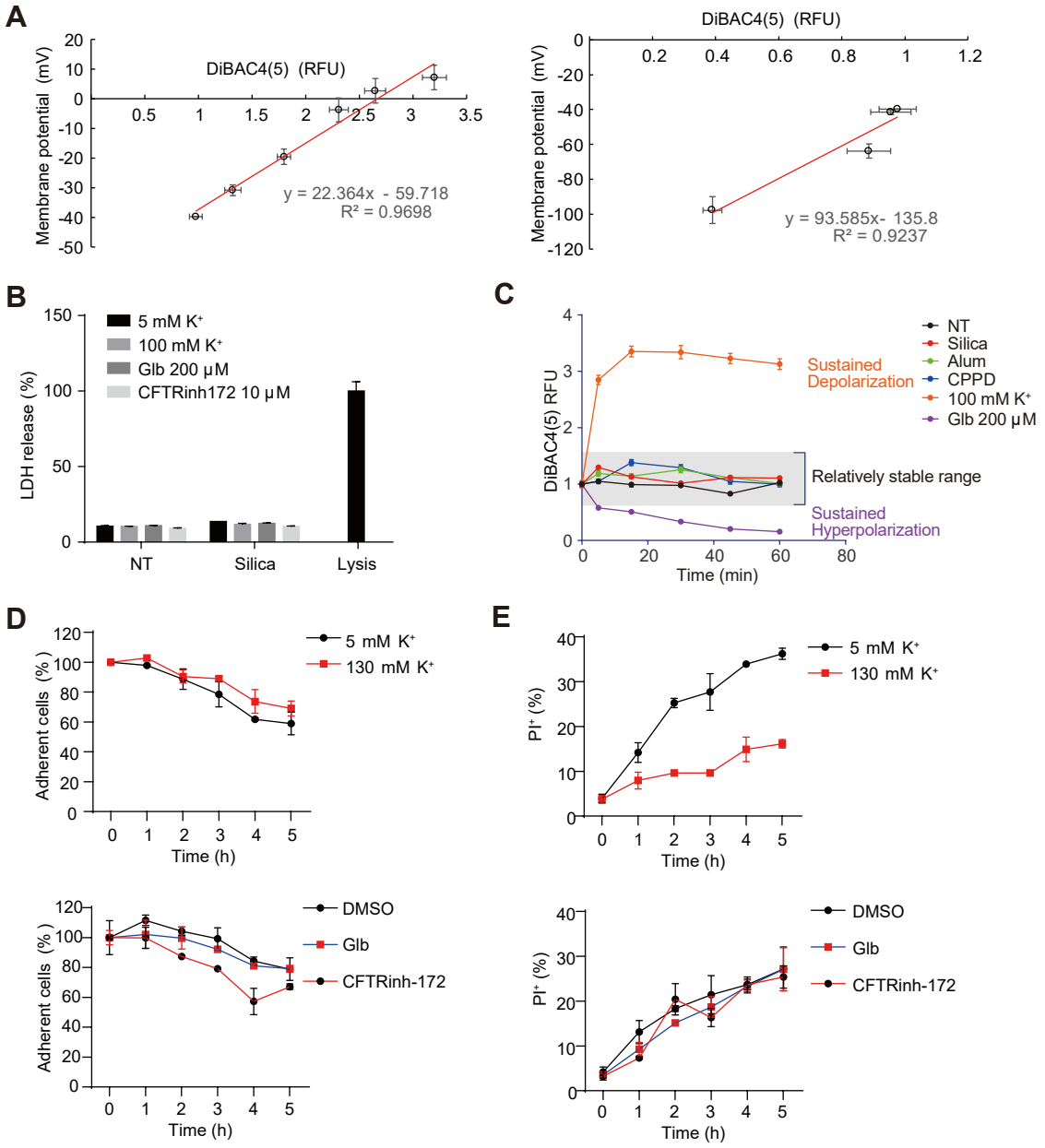

Figure S3. The MP is maintained close to the resting value for NLRP3 inflammasome activation, related to Figure 3.

(A) DiBAC4(5) staining intensity in THP-1 macrophages was calibrated to MP based on the patch clamping data under different concentrations of extracellular K^+ (left) or glyburide (right). (B) THP-1 cells treated as indicated for 1h and cell death was measured by LDH cytotoxicity detection kit (n=3). (C) DiBAC4(5) RFU Changes over time in THP-1 macrophages under different stimuli was measured by DiBAC4(5) staining. Results are pool of 3 independent experiments. (D, E) THP-1 cells were treated with silica under indicated conditions for different times and then were washed as we did for the K^+ content measurement assay. Remaining adherent cell numbers (D) were counted by Flow cytometric analysis and cell death (E) was analyzed by propidium iodine (PI) staining (n=3). Data are shown as mean ± SEM and are representative of two independent experiments (D, E).

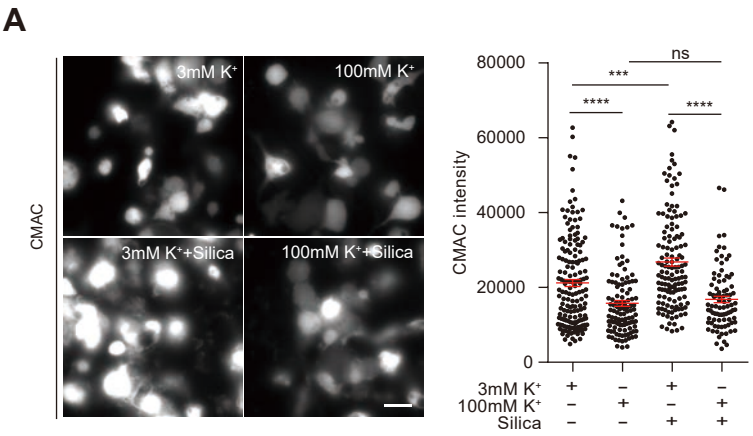

Figure S4. Disruption of membrane potential causes calpain activity attenuation in BMDCs, related to Figure 4. (A) Calpain activity in BMDCs treated with indicated stimuli were measured by CMAC. Scale bar is 20 μm. Right panels: plots of intensities of CMAC fluorescence in individual cells. ns, not significant. *** $p<0.001$, **** $p<0.0001$. Data are representative of two independent experiments.

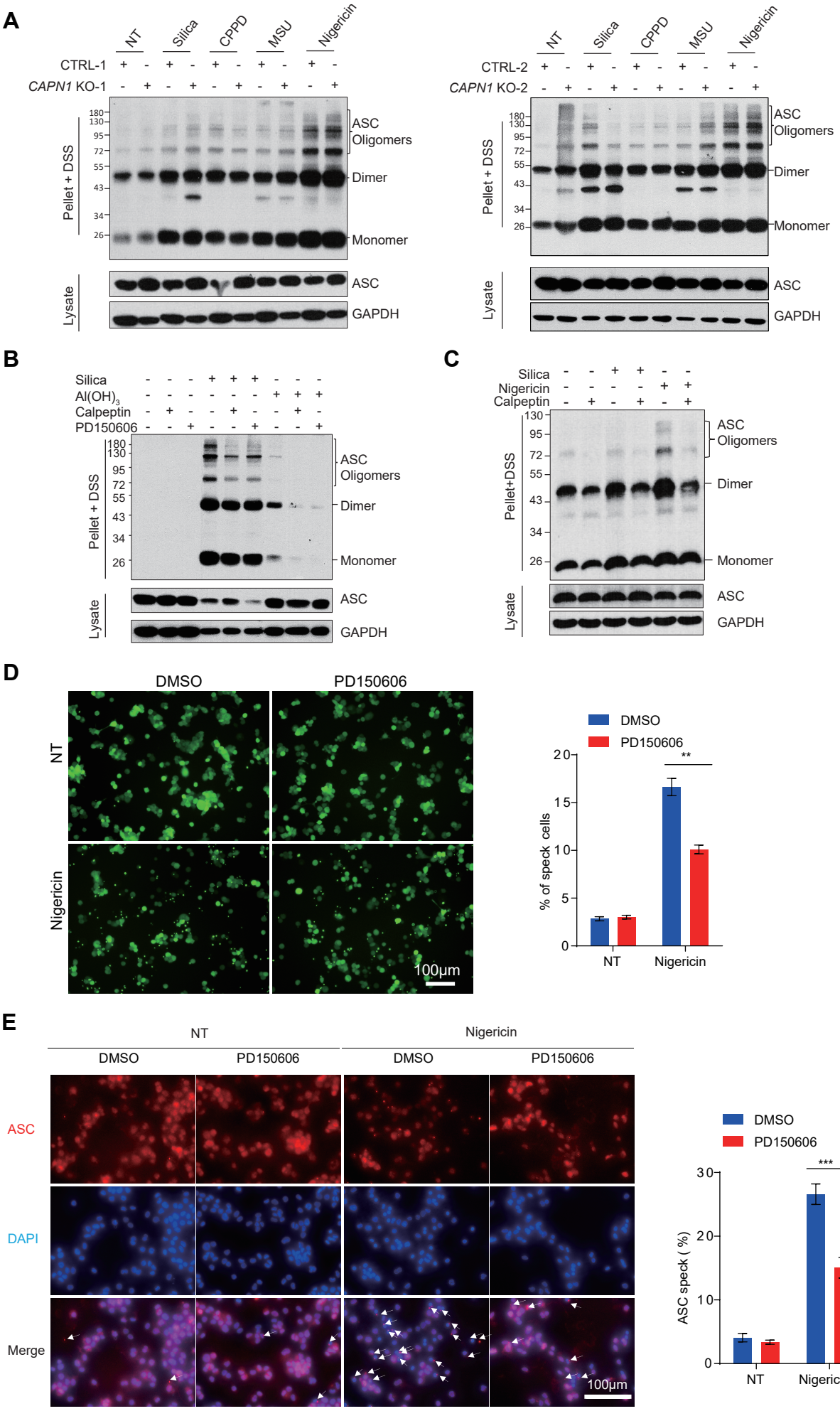
A
NT
Silica
CPPD
MSU
Nigericin
CTRL-1
CAPN1 KO-1
CTRL-2
CAPN1 KO-2
Pellet + DSS
Lysate
ASC
Oligomers
Dimer
Monomer
GAPDH
B
Silica
Al(OH)3
Calpeptin
PD150606
C
Nigericin
Pellet+DSS
D
DMSO
PD150606
NT
Nigericin
100μm
% of speck cells
E
ASC
DAPI
Merge
ASC speck (%)

Figure S5. μ-calpain regulates signals downstream of ASC oligomerization while other calpain species regulate upstream signals, related to Figure 6.
(A-C) Two CAPN1 knockout THP-1 cells lines (A), BMDMs (B) or THP-1 cells (C) were treated as indicated. The triton X-100 insoluble pellets were cross-linked with DSS, and analyzed by ASC immunoblotting. Data are representative at least 2 independent experiments. (D) Representative images and quantification of ASC speck formation upon NLRP3 stimulation in EGFP-ASC THP-1 macrophages. (E) Endogenous ASC was stained by immunofluorescence in THP-1 macrophages. Representative images and quantification of ASC speck formation were shown. For (D) and (E), more than 6 random images from 3 independent experiments were analyzed. Bar, 100 μm.

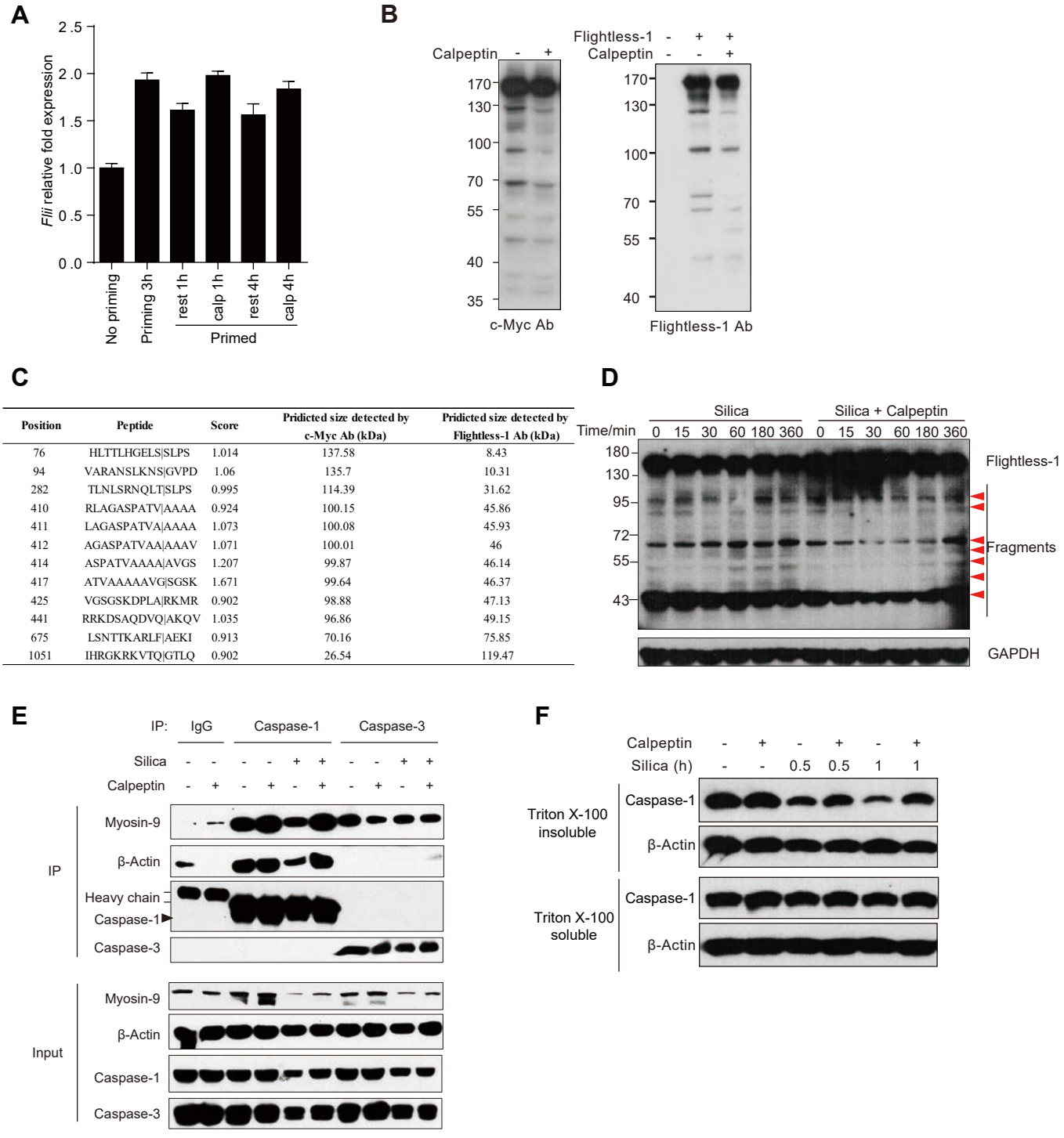

Position	Peptide	Score	Pridicted size detected by c-Myc Ab (kDa)	Pridicted size detected by Flightless-1 Ab (kDa)
76	HLTTLHGELS|SLPS	1.014	137.58	8.43
94	VARANSLKNS|GVPD	1.06	135.7	10.31
282	TLNLSRNQLT|SLPS	0.995	114.39	31.62
410	RLAGASPATV|AAAA	0.924	100.15	45.86
411	LAGASPATVA|AAAA	1.073	100.08	45.93
412	AGASPATVAA|AAAV	1.071	100.01	46
414	ASPATVAAAA|AVGS	1.207	99.87	46.14
417	ATVAAAAAVG|SGSK	1.671	99.64	46.37
425	VGSGSKDPLA|RKMR	0.902	98.88	47.13
441	RRKDSAQDVQ|AKQV	1.035	96.86	49.15
675	LSNTTKARLF|AEKI	0.913	70.16	75.85
1051	IHRGKRKVTQ|GTLQ	0.902	26.54	119.47

Figure S6. Removal of Caspase-1 inhibition by flightless-1 and actin sequestration requires Ca^{2+} activated calpain, related to Figure 6.

(A) LPS-primed BMDCs were treated with calpeptin for 1 or 4 hrs. Flightless -1 mRNA fold change was analyzed by q-PCR. (B) C-terminal myc-tagged Flightless-1 was transfected in 293FT cells and calpeptin was added 8 hrs after the transfection. At 24 hrs, Triton X-100-insoluble fraction proteins were extracted for Western blot with Flightless-1 antibody (recognize N-terminal 300aa) or c-myc antibody. (C) 52 calpain cut sites on mouse Flightless-1 are predicted by GPS-CCD 1.0 when the threshold was set at high level (cutoff 0.654). Shown are partial examples of predicted calpain cleavage sites (score>0.902) and their corresponding sizes detected by c-terminal myc or Flightless-1 antibody. (D) WB analysis of Flightless-1 in BMDCs treated with silica. (E) BMDMs were treated with silica in the presence or absence of calpeptin for 1h and lysates were immunoprecipitated with anti-Caspase-1 or anti-Caspase-3 antibodies, and detected by myosin-9 and β actin antibodies. (F) BMDMs were treated as indicated and then lysed in Triton buffer. Bundled F -actin pool (triton X-100 insoluble) were enriched in low-speed pellet and subjected to immunoblotting. Data are representative of 2 or 3 independent experiments.

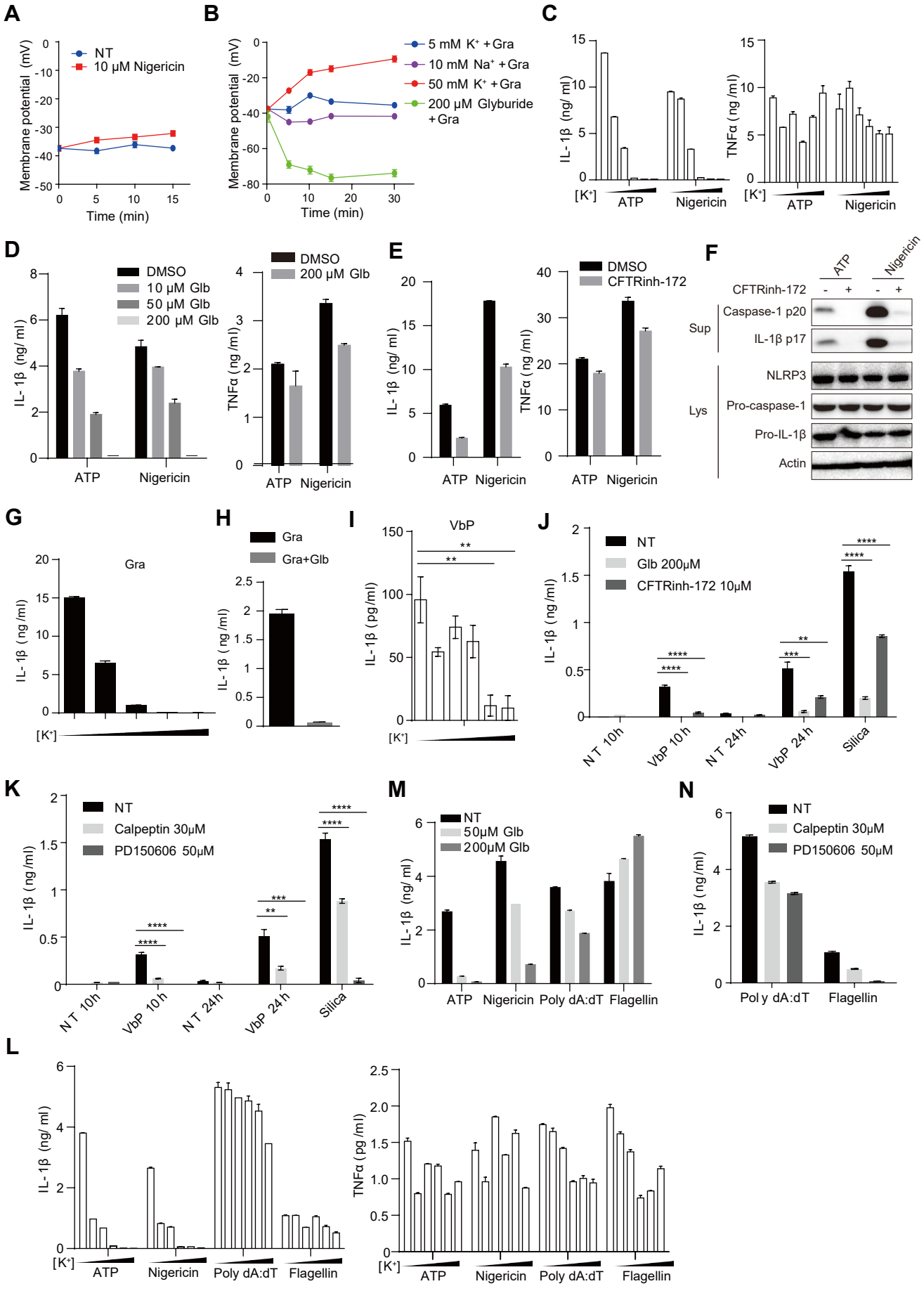
A
Membrane potential (mV)
Time (min)
NT
10 μM Nigericin
B
Membrane potential (mV)
Time (min)
5 mM K+ +Gra
10 mM Na+ +Gra
50 mM K+ +Gra
200 μM Glyburide +Gra
C
IL-1β (ng/ ml)
TNFα (ng /ml)
[K+]
ATP
Nigericin
D
DMSO
10 μM Glb
50 μM Glb
200 μM Glb
IL-1β (ng/ ml)
TNFα (ng /ml)
ATP
Nigericin
E
DMSO
CFTRinh-172
IL-1β (ng/ ml)
TNFα (ng /ml)
ATP
Nigericin
F
ATP
Nigericin
CFTRinh-172
Sup
Caspase-1 p20
IL-1β p17
Lys
NLRP3
Pro-caspase-1
Pro-IL-1β
Actin
G
Gra
IL-1β (ng /ml)
[K+]
H
Gra
Gra+Glb
IL-1β (ng /ml)
I
VbP
IL-1β (pg/ml)
[K+]
J
NT
Glb 200μM
CFTRinh-172 10μM
IL-1β (ng/ml)
NT 10h
VbP 10h
NT 24h
VbP 24h
Silica
K
NT
Calpeptin 30μM
PD150606 50μM
IL-1β (ng/ml)
NT 10h
VbP 10h
NT 24h
VbP 24h
Silica
M
NT
50μM Glb
200μM Glb
IL-1β (ng/ ml)
ATP
Nigericin
Poly dA:dT
Flagellin
N
NT
Calpeptin 30μM
PD150606 50μM
IL-1β (ng/ml)
Poly dA:dT
Flagellin
L
IL-1β (ng/ ml)
TNFα (pg /ml)
[K+]
ATP
Nigericin
Poly dA:dT
Flagellin

Figure S7. The near resting state MP contributes to non-crystal induced NLRP3 activation and non-NLRP3 inflammasome activation, related to Figure 2 and Figure 3.

(A) MP changes under nigericin treatment in THP-1 cells were measured by DiBAC4(5) staining. (B) THP-1 cells were treated with gramicidin (Gra) in normal medium (5 mM K^+), low Na^+ medium (10 mM Na^+) in which Na^+ was substituted by the membrane impermeable cation choline, 50 mM K^+ medium or glyburide medium, and MP changes were detected by DiBAC4(5) staining. (C-E) BMDCs were pretreated with increasing concentrations of extracellular K^+ (5, 10, 20, 50, 75 and 100 mM) (C), glyburide (D) or 10 μM CFTRinh-172 (E), and then treated with ATP or nigericin for 1 hr. IL -1β and TNFα production were measured by ELISA. (F) Immunoblot of activated Caspase-1 and mature IL-1β in supernatants and all NLRP3 inflammasome components in cell lysates of BMDMs. (G, H) THP-1macrophages were pretreated with increasing concentrations of extracellular K^+ (5, 20, 40, 75 and 100 mM) (G) or 200 μM glyburide (H) and then treated with gramicidin for 1 hr. IL-1β production was measured by ELISA. (I-K) BMDMs were pretreated with increasing levels of extracellular K^+ (5, 10, 20, 50, 75 and 100 mM, left to right) (I), glyburide or CFTRinh-172 (J), Calpeptin or PD150606 (K), and then treated with 20 μM Val-boroPro (VbP) for 10 hrs or 24 hrs. IL-1β releasing was measured by ELISA. (L-N) BMDMs were pretreated with increasing levels of extracellular K^+ (5, 10, 20, 50, 75 and 100 mM, left to right) (L), glyburide (M), Calpeptin or PD150606 (N), and then treated with ATP, nigericin or transfected with poly dA:dT or flagellin. IL-1β and TNFα releasing was measured by ELISA. Data are shown as mean ± SEM and represents at least 2 independent experiments.

Table S1. MS identified Caspase-1 binding proteins with large difference in MS hit numbers between Silica 1h and Silica 1h+Calpeptin treatments, related to Figure 6.

#	Identified Proteins	Molecular Weight	Total Spectrum Count		Function
			Silica 1h	Silica 1h +calpeptin	
1*	myosin-9	226 kDa	8	52	Cytoskeleton reorganization, focal contacts formation
2*	actin, cytoplasmic 1	42 kDa	9	38	Actin cytoskeleton
3	vimentin	54 kDa	3	34	Type III intermediate filament
4	unconventional myosin-If	125 kDa	0	18	Actin-based motor molecules
5	plectin isoform 12alpha	534 kDa	0	16	Organizers of intermediate filament cytoarchitecture. Harbors a functional actin-binding domain.
6	ras GTPase-activating-like protein IQGAP1	189 kDa	0	15	Reorganization of the actin cytoskeleton at the plasma membrane.
7	galectin-3	27 kDa	8	14	β-galactoside-binding protein. Plays an important role in cell-cell adhesion, cell-matrix interactions.
8	desmoplakin	333 kDa	2	11	Maintain the structural integrity at adjacent cell contacts.
9	unconventional myosin-Ie	127 kDa	0	10	Actin-based motor molecules
10	annexin A7	50 kDa	6	10	Calcium-dependent phospholipid binding protein
11	unconventional myosin-Ig	119 kDa	0	9	Actin-based motor molecules
12	junction plakoglobin	82 kDa	4	8	The only known constituent common to submembranous plaques of both desmosomes and intermediate junctions.
13	unconventional myosin-Ic isoform a	120 kDa	0	7	Actin-based motor molecules
14	aminopeptidase N	110 kDa	3	7	Digestion of peptides generated from hydrolysis of proteins by gastric and pancreatic proteases
15	actin-related protein 3	47 kDa	1	6	Functions as ATP-binding component of the Arp2/3 complex
16	EF-hand domain-containing protein D2	27 kDa	0	5	Negative regulator of the canonical NF-kappa-B-activating branch.
17	F-actin-capping protein subunit beta isoform d, CAPZB	29 kDa	0	5	Cytoskeletal organization
18	elongation factor 1-alpha 1, eEF1A1	50 kDa	0	5	Protein biosynthesis. Interact with cytoskeleton.
19	flightless-1	145 kDa	0	5	Coactivator in transcriptional activation. Cytoskeletal rearrangement.

Continue

20	coronin-1C	53 kDa	0	5	Contain actin binding domain and may be involved in cytokinesis, motility and signal transduction.
21	unconventional myosin-XVIIIa	231 kDa	0	4	Actin-based motor molecules
22	78 kDa glucose-regulated protein precursor	72 kDa	0	3	Involved in the correct folding of proteins.
23	annexin A11	54 kDa	0	2	Involved in midbody formation and cytokinesis.
24	gelsolin	86 kDa	0	2	A key regulator of actin filament assembly and disassembly.
25	heat shock cognate 71 kDa protein	71 kDa	0	2	A repressor of transcriptional activation. Component of the PRP19-CDC5L splicing complex.
26	E3 ubiquitin-protein ligase TRIM21	53 kDa	0	2	Regulate ubiquitination and cell cycle progression.
27	filamin-A	280 kDa	0	2	Actin binding protein. Regulates reorganization of the actin cytoskeleton .
28	prelamin-A/C	65 kDa	0	2	Nuclear assembly and chromatin organization.
29	actin-related protein 2/3 complex subunit 1B, ARPC1B	41 kDa	0	2	A subunit of the Arp2/3 protein complex that plays a major role in the regulation of the actin cytoskeleton.
30	alpha-actinin-4	105 kDa	0	2	F-actin cross-linking protein
31	transitional endoplasmic reticulum ATPase	89 kDa	0	2	Involved in the formation of the transitional endoplasmic reticulum.
32	lysosome-associated membrane glycoprotein 2	46 kDa	0	2	Protect the lysosomal membrane.
33	Predicted: biliverdin reductase A isoform X3	23 kDa	0	2	A scaffold and intracellular transporter of kinases that regulate growth and proliferation of cells.
34	peroxiredoxin-1	22 kDa	0	2	Antioxidant enzyme
35	14-3-3 protein zeta/delta	28 kDa	0	2	Bind and modulate a large number of partners, usually by recognition of a phosphoserine or phosphothreonine motif.

* Main visible bands are cut off from Coomassie blue gel.